DE GRUYTER OPEN

Int. J. of Applied Mechanics and Engineering, 2015, vol.20, No.1, pp.127-145
DOI: 10.1515/ijame-2015-0009

THE DYNAMIC CHARACTERISTIC AND HYSTERESIS EFFECT OF AN AIR SPRING

F. LÖCKEN* and M. WELSCH
Helmut-Schmidt-Universität:
Institut für Maschinenelemente und Rechnergestützte Produktentwicklung
Holstenhofweg 85, 22043 Hamburg, GERMANY
E-mail: florian.loecken@hsu-hh.de
michael.welsch@hsu-hh.de

In many applications of vibration technology, especially in chassis, air springs present a common alternative to steel spring concepts. A design-independent and therefore universal approach is presented to describe the dynamic characteristic of such springs. Differential and constitutive equations based on energy balances of the enclosed volume and the mountings are given to describe the nonlinear and dynamic characteristics. Therefore all parameters can be estimated directly from physical and geometrical properties, without parameter fitting. The numerically solved equations fit very well to measurements of a passenger car air spring. In a second step a simplification of this model leads to a pure mechanical equation. While in principle the same parameters are used, just an empirical correction of the effective heat transfer coefficient is needed to handle some simplification on this topic. Finally, a linearization of this equation leads to an analogous mechanical model that can be assembled from two common spring- and one dashpot elements in a specific arrangement. This transfer into "mechanical language" enables a system description with a simple force-displacement law and a consideration of the non-obvious hysteresis and stiffness increase of an air spring from a mechanical point of view.

Key words: air springs, dynamic characteristic, transfer thermodynamic to mechanic.

1. Introduction

Air springs have become established in vibration isolation applications in industrial facilities and in chassis with the requirement of a load-independent working level. Figure 1 gives an overview of different types of air springs. By controlling the internal pressure, the reaction force can be adjusted to keep a constant height level. The stiffness and the vibration behavior can be designed independently from the preload force. This is a great advantage compared to steel spring concepts, where a compromise has to be chosen in this regard. During the suspension process the air volume (enclosed between the bellows and mounting elements) undergoes a thermodynamic change of state, which leads to a heat transfer. As mentioned in Kornhauser and Smith (1993), Kornhauser (1994) for gas springs, this causes a hysteresis in the characteristic and stiffness-increase in a specific frequency range. Figure 2 shows three measured characteristics within this range. The arising of hysteresis is evidently for the middle characteristic curve. The rise of the peak forces, due to the increasing stiffness becomes obvious in the two characteristic curves of the higher frequencies.

This work estimates the dynamic behavior by the principle of energy balances. This approach is not entirely new and has already been formulated by Pelz and Buttenbender (2004), but just for an idealized air spring. Therefore no force- displacement equations were given to model real air springs. The authors concluded that the ratio between the two boundary stiffnesses for isothermal and adiabatic change of state must be the same as the isentropic exponent $\kappa = 1.4$ of air. As becomes apparent, in general this factor depends on the geometry of the mounting elements. For passenger car air springs it lies between 1.2 and 1.6.

* To whom correspondence should be addressed

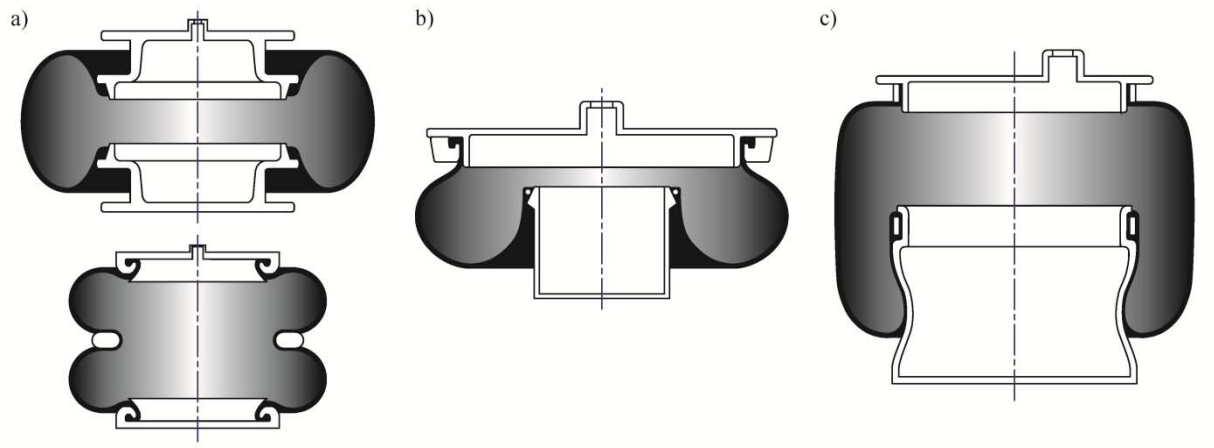

Fig.1. Overview of air spring types following (Voß, 1988): (a) convoluted air spring; (b) unrestricted air spring; (c) rolling lobe airspring.

However, the most common derivation for modeling an air spring deals with an equilibrium of forces (Chang, 2008; Quaglia and Sorli, 2001; Schützner *et al*., 1994) where the thermodynamics is simply considered by the change of pressure. In general, this assumption leads to models with limited validity for dynamic issues. With such an approach the thermodynamics and the bellow elasticity are irregular superimposed, by defining a so-called effective area. Further an irregular fitting of the physically constrained isentropic exponent of air is used in practice to match measurements.

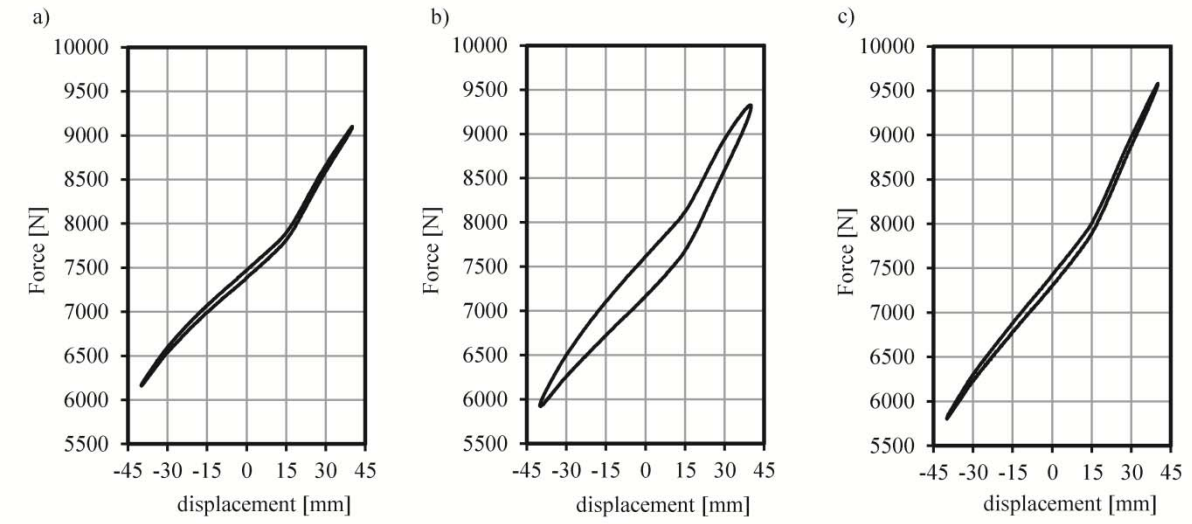

Fig.2. Air spring characteristic curves measured for different frequencies: (a) *0.001* Hz; (b) *0.022* Hz; (c) *1.024* Hz (N.N., Int. doc. Trelleborg Vibracoustic, 2013).

In all these models the differential, physical correlation between the displacement area and volume are not taken into account. This observation was first introduced by Welsch (2007) who gives a force-displacement law for the isothermal and adiabatic special cases with splitting the system into pure thermodynamic stiffness and the bellow elasticity. Massmann (1995) calculated the volume compression and

the bellow elasticity with a coupled continuum approach via FEM. However the dynamics of heat exchange are still ignored.

This work focuses on the explanation and prediction of the thermodynamic part of the air spring stiffness. A new derivation of the energy balances is presented. It expands the energy balance principle of Pelz and Buttenbender with the superimposing approach of Welsch. In addition, it takes the heat transfer and storage in the mountings into account. This enables a design-independent and therefore universal approach to describe the non-linear dynamic characteristic of air-springs by differential and constitutive equations. Therefore all parameters can be estimated directly from physical and geometrical properties, without parameter fitting.

Simplifications of the heat transfer and a constitutive assumption about the volume change as a function of displacement lead to a pure mechanical equation. While in principle the same parameters are used, just an empirical correction of the effective heat transfer coefficient is needed to handle some simplifications on this topic.

Further, a linearization of the equations gives rise to a mechanical three-parameter model, consisting of two spring elements and one dashpot element. This transfer into ”mechanical language” enables a linear system description with a simple force- displacement law that can be analytically solved in the frequency domain. The parameters of this mechanical three-parameter model can be directly expressed by the thermodynamic and geometric parameters of the enclosed air volume.

Finally, the dynamic system behavior of a passenger car air spring is simulated to estimate the validity of the given approach. The numerically solved non-linear thermodynamic model fits very well to measurements. Because the mechanical three- parameter model corresponds to linearization, the non-linear characteristic disappears, but the prediction of the hysteresis and stiffness increase is still accurate.

2. Air spring models

2.1. Non-linear thermodynamic basic equations

Figure 3 shows an air spring in design-position and deflected position, including the state variables of the enclosed air and the heat flows. The spring is divided into two control volumes to determine the energy interaction between the enclosed air, the mounting elements (incl. the bellows) and the environment.

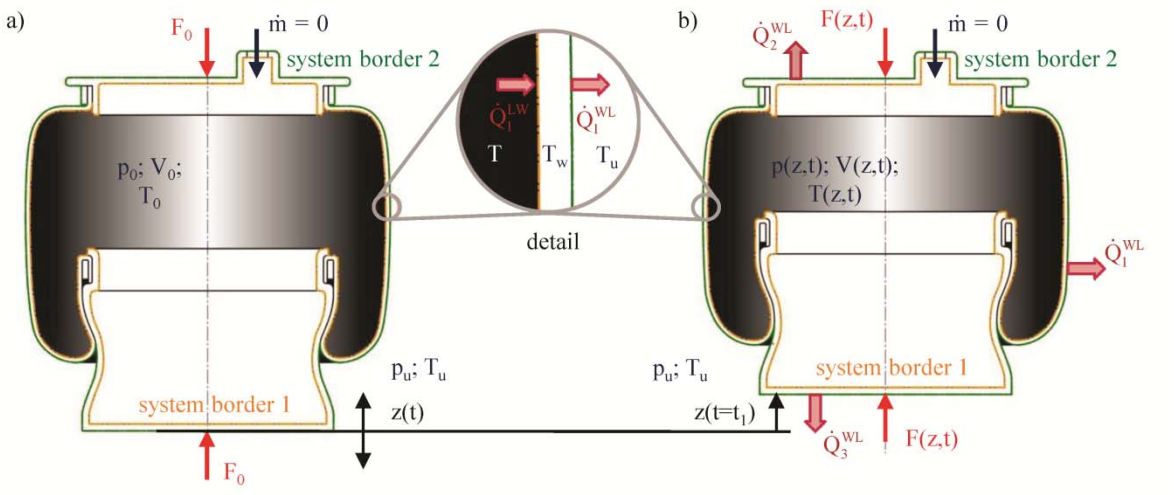

Fig.3. System borders of the control volumes of an air spring in (a) design-position and (b) deflected condition.

The first control volume corresponds to the air volume enclosed in the spring and is termed system 1 in what follows. The other system border runs along the outer contour of the spring, so the mounting elements and the rolling lobe are merged in one control volume (system 2).

The balance of the internal energy as scalar formulation of the first law of thermodynamics describes the process of heat conversion, i.e., the conversion of kinetic energy into internal energy

$$\frac{dU}{dt} = \sum \frac{dQ}{dt} + \sum P_{ext} + \sum_{in} \frac{dm_{in}}{dt}\left(h_{in} + \frac{{c_{in}}^2}{2} \right) - \sum_{out} \frac{dm_{out}}{dt}\left(h_{out} + \frac{{c_{out}}^2}{2} \right). \tag{2.1}$$

The time change of the inner energy state $dU/dt = \dot{U}$ is the sum of the heat flows transported across the system border $dQ/dt = \dot{Q}$, a general external power transfer P_{ext} and the energy change caused by the material transport $\left(dm_{in}/dt = \dot{m}_{in}, dm_{out}/dt = \dot{m}_{out} \right)$.

Usually the air volume (system 1) is closed, so no material transport occurs between the systems $\left(\dot{m} = 0 \right)$, but heat can be transported across the system borders.* Consequently, the general energy balance is reduced to

$$\dot{U} = \sum \dot{Q} + \sum P_{ext}. \tag{2.2}$$

According to the second law of thermodynamics, heat flows in the direction of the temperature gradient. Fourier's law for one-dimensional heat conduction is defined by

$$\dot{Q} = -\alpha A_w \left(T - T_w \right) \qquad \text{for} \qquad T > T_w, \tag{2.3}$$

with the effective surface A_w at the system border and the heat transfer coefficient α. The general power term P_{ext} for the air volume can be expressed by the relationship

$$P_{ext} = -p\dot{V} \tag{2.4}$$

where $\dot{V} = dV/dt$ is the time change of the volume and p is the hydrostatic pressure within the volume. In general, an amount of potential energy is stored in the fiber-reinforced bellow and the mounting elements. However, they cannot be directly reduced to a scalar formulation, so they are disregarded in this work. The stiffness components of the bellow can be added separately by superimposing a parallel stiffness to the air spring for a decoupled approach.

For expected temperature changes of less than $\pm 100\,K$, the changes of the inner energies $\dot{U}$ can be described for both systems by constant isochoric heat capacities c_v for the air volume and c_i for the mounting elements

* The mass flows become relevant in balance equations of filling processes or systems with several volumes, such as air spring dampers (ASD). Consideration of such multi-volume systems can be found, e.g., in the works of Pelz *et al.* (2002), Pelz (2007) and Lee and Kim (2007).

$$\dot{U}_L = m_L c_v \dot{T} \quad \text{(air volume)},$$
$$\sum_{i=1}^{n} \dot{U}_i = \sum_{i=1}^{n} m_i c_i \dot{T}_{wi} \quad \text{(mounting elements)} \tag{2.5}$$

with $\dot{T}$ or $\dot{T}_{wi}$ for the changes of the inner temperatures and m_L or m_i for the constant masses.[†] The index n indicates the number of components integrated in system 2.

Due to the low wall thicknesses of the mounting elements the effective surfaces and transfer coefficients during heat transport can be assumed to be of equal size for both system borders. With the ambient temperature T_u and the flow direction of the heat, Eq.(2.2) to Eq.(2.5) can be summarized as

$$m_L c_v \dot{T} + p\dot{V} + \sum_{i=1}^{n} \alpha_i A_{wi} \left(T - T_{wi}\right) = 0 \quad \text{(air volume)},$$
$$\sum_{i=1}^{n} m_i c_i \dot{T}_{wi} + \sum_{i=1}^{n} \alpha_i A_{wi} \left(2T_{wi} - T - T_u\right) = 0 \quad \text{(mounting elements)}. \tag{2.6}$$

Hence the air spring is described by two (non-linear) differential equations, which are coupled to each other due to the heat transport via the temperatures T and T_{wi}. System 2 denotes an additional energy store, which is important to predict the correct frequency range of the hysteresis.

2.2. Non-linear mechanical model with simplified heat transfer

To transfer Eq.(2.6) to a pure mechanical model it is assumed that the components are thin in the sense of heat transfer and thermal storage in the mounting elements can be neglected. Consequently, the individual heat transfers through the mounting elements are merged in one effective heat flow $\dot{Q}_{eff} = -kA\left(T - T_u\right)$ and Eq.(2.6) can be reduced to

$$m_L c_v \dot{T} + p\dot{V} + kA\left(T - T_{wi}\right) = 0, \tag{2.7}$$

with $kA = \sum k_i A_i$.

In this context, the defined heat transmission coefficient kA is the sum of the transfer and transmission coefficients of individual mounting elements $k_i A_i$. The inverse heat transmission coefficients $1/k_i A_i$ are composed of the serially connected transfer resistances

$$\frac{1}{k_i A_i} = \frac{1}{\alpha_1^i A_1^i} + \frac{\delta_i}{\lambda_m^i A_m^i} + \frac{1}{\alpha_2^i A_2^i}. \tag{2.8}$$

[†] In general, the heat capacity of gases depends on the temperature, but can be assumed to be constant here on account of the slight temperature changes. The following applies to air: $c_v(173K) = 0.722 kJ/kgK$ and $c_v(373K) = 0.725 kJ/kgK$ Baehr (2008).

Here α_1^i and α_2^i describe the heat transfer coefficients on the surfaces A_1^i, A_2^i and $\delta_i \big/ \left(\lambda_m^i A_m^i\right)$ describes the heat transmission resistance of the component with the wall thickness δ_i, the heat conductivity λ_m^i and the average area A_m^i. The air can be described by the ideal gas law for the expected temperatures

$$pV = m_L RT. \tag{2.9}$$

With the derivation $\dot{T} = \left(\dot{p}V + p\dot{V}\right) \big/ \left(m_L R\right)$ and $R/c_v = (\kappa - 1)$, with the isotropic exponent κ, the gas constant *R* and the specific heat capacity c_v, Eq.(2.7) can be reduced to the absolute variables pressure *p* and volume *V*

$$\dot{p} + p\left[\kappa \frac{\dot{V}}{V} + K_1\right] - \frac{K_2}{V} = 0, \tag{2.10}$$

with $K_1 = \dfrac{kA}{m_L c_v}$ and $K_2 = (\kappa - 1)kAT_u$.

Hence, the inner temperature *T* is eliminated. In the next steps the thermodynamic variables $p(t)$, $\dot{p}(t)$, $V(t)$, $\dot{V}(t)$ must be substituted with the mechanical variables: force $F(t)$, displacement $z(t)$ and their time changes $\dot{F}(t)$, $\dot{z}(t)$. The absolute pressure *p* within the spring and the constant ambient pressure p_u are coupled with the force via the differential work $dW = -\left(p - p_u\right)dV$. Using the abbreviation $dV/dz = V'$ the spring force can be expressed as

$$F = -\left(p - p_u\right)V'. \tag{2.11}$$

As a result, the spring force is a function of the absolute pressure, the ambient pressure and the change of the volume: $F = f\left(p, p_u, V'\right)$. To insert Eq.(2.11) in Eq.(2.10), the volume change and displacement must be brought into a direct functional connection. To keep the balance equation generally valid for different spring types, only the constitutive assumption is made that the spring volume is exclusively a function of the displacement: $V = V(z)$ and does not depend on other variables. In general, the volume is affected by pressure change, depending on the elasticity of the bellow. However, the bellow elasticity was disregarded, so this assumption seems to be consequent in this case. A Taylor-series expansion around the design- position $\left(z = 0\right)$ leads to

$$V(z) = V_0 + \sum_{n=1}^{\infty} \frac{1}{n!} \frac{d^n V}{dz^n}\bigg|_{z=0} z^n = V_0 + V_1 z + \frac{1}{2} V_2 z^2 + \frac{1}{6} V_3 z^3 \ldots \tag{2.12}$$

with the coefficients $V_n = \left(V_1, V_2, V_3 \ldots\right) = d^n V / dz^n \big|_{z=0}$.

Assuming a rotationally symmetrical design of the spring, the change of volume is primarily defined by the rolling of the bellow on the mountings. The geometric interpretation and estimation of the volume coefficients $\left(V_1, V_2, V_3 \ldots\right)$ is quite extensive and therefore not examined in more detail at this point. The

polynomial form of the Taylor expansion gives the possibility to describe the time derivations of the variables V and V' by the displacement velocity $\dot{z}$

$$\frac{dV}{dt}=\dot{V}=V'\dot{z}=\left(V_1 z+\frac{1}{2}V_2 z^2+\frac{1}{6}V_3 z^3+\ldots\right)\dot{z},$$

$$\frac{d(V')}{dt}=\dot{V}'=V''\dot{z}=\left(V_2 z+\frac{1}{2}V_3 z^2+\ldots\right)\dot{z}, \tag{2.13}$$

$$\vdots$$

$$\text{general}:\frac{d\left(\frac{d^n V}{dz^n}\right)}{dt}=\left(\frac{d^{n+1}V}{dz^{n+1}}\right)\dot{z}.$$

Equation (2.10) can now be expressed as a function of force and displacement

$$\dot{F}+F\left[\left(\kappa\frac{V'}{V}-\frac{V''}{V'}\right)\dot{z}+K_1\right]-p_u V'\left(\kappa\frac{V'}{V}\dot{z}+K_1\right)+K_2\frac{V'}{V}=0. \tag{2.14}$$

Consequently, the time derivation of the force is a function of the displacement, velocity and force itself: $\dot{F}=f\left(F,z,\dot{z}\right)$.

2.3. Linearized mechanical model with simplified heat transfer

By neglecting the mounting elements as heat storage, using the ideal gases law (see Eq.(2.9)) and a decoupled equation of the bellows volume (see Eq.(2.12)), the differential equation system in Eq.(2.5) is reduced to an inhomogeneous differential equation of first order (see Eq.(2.14)). As a result, the thermodynamic behavior of an air spring, including the non-linearity of the characteristic curve, is transferred to a mechanical model. Unfortunately, this differential equation cannot be solved analytically. In order to be able to estimate the dynamic system behavior without numerical applications, Eq.(2.14) must be converted into a linear differential equation around a stationary position of equilibrium (working point WP).

The air spring is in a stationary state if the displacement $z(t)$ and the force $F(t)$ do not undergo any time change $\left(\dot{F},\dot{z}=0\right)$. With regard to Eq.(2.14), this condition is valid for every displacement $z(t)=\text{const.}$. Hence, the design-position $z=0$ is selected for the linearization: $\boldsymbol{x_0}=\left(\dot{F}_0 \quad F_0 \quad \dot{z}_0 \quad z_0\right)^T=$ $=\left(0 \quad F_0 \quad 0 \quad 0\right)^T$. The variable F_0 describes the static preload of the spring that corresponds to the weight acting on the spring. The linearization is given by $f(\boldsymbol{x})\approx\boldsymbol{J}(\boldsymbol{x_0})\Delta\boldsymbol{x}$ with the Jacobian matrix: $\boldsymbol{J}(\boldsymbol{x_0})=\left[\partial f/\partial\dot{F}\big|_{\boldsymbol{x_0}} \quad \partial f/\partial F\big|_{\boldsymbol{x_0}} \quad \partial f/\partial\dot{z}\big|_{\boldsymbol{x_0}} \quad \partial f/\partial z\big|_{\boldsymbol{x_0}}\right]$. It contains the partial derivations of the differential equation $f(\boldsymbol{x})$ according to the time-changing variables $\boldsymbol{x}$ at the point $\boldsymbol{x_0}$. Hence, the linearized form of Eq.(2.14) can be expressed by the following equation

$$J_1\dot{F}+J_2\left(F-F_0\right)+J_3\dot{z}+J_4 z=0, \tag{2.15}$$

with the coefficients of the Jacobian matrix

$$J_1 = \left.\frac{\partial f}{\partial \dot{F}}\right|_{x_0} = 1,$$

$$J_2 = \left.\frac{\partial f}{\partial F}\right|_{x_0} = K_1,$$

$$J_3 = \left.\frac{\partial f}{\partial \dot{z}}\right|_{x_0} = -\kappa p_u \frac{V_1^2}{V_0} + F_0\left(\kappa\frac{V_1}{V_0} - \frac{V_2}{V_1}\right),$$

$$J_4 = \left.\frac{\partial f}{\partial z}\right|_{x_0} = -K_1 p_u V_2 + K_2\left[\frac{V_2}{V_0} - \left(\frac{V_1}{V_0}\right)^2\right].$$

Since both the series expansion of the volume function and linearization occur around the expansion point $z = 0$, the terms V, V', V'' are reduced within the Jacobian coefficients to the constant volume parameters V_0, V_1, V_2 from Eq.(2.12). The variables K_1 and K_2 correspond to the coefficients in Eq.(2.10). Eq.(2.15) is well known in the linear system theory and can be interpreted as a mechanical analogous model as shown in Fig.4. It consists of the parallel connection of a linear spring element with the coefficient c_0 and a Maxwell element, consisting of a serial connection of a spring element with the coefficient c_1 and a linear dashpot element with the coefficient *b*.

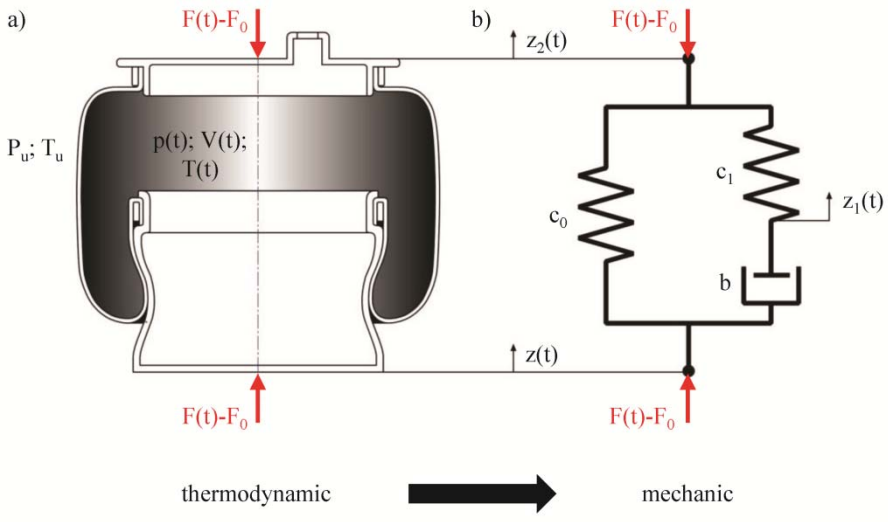

Fig.4. Comparison of (a) thermodynamical model and (b) mechanical analogous model for an air spring.

This arrangement can be deduced from force equilibrium in a familiar way with two coupled equations

$$F - F_0 = c_0\left(z - z_2\right) + c_1\left(z_1 - z_2\right),$$
$$c_1\left(z_1 - z_2\right) = b\left(\dot{z} - \dot{z}_1\right) \tag{2.16}$$

leading to

$$F - F_0 + \frac{b}{c_1}\dot{F} + c_0 z_2 + b\left(1 + \frac{c_0}{c_1}\right)\dot{z}_2 = c_0 z + b\left(1 + \frac{c_0}{c_1}\right)\dot{z}. \tag{2.17}$$

Further, this equation can be reduced by local consideration $\left(z_2 = 0\right)$ to

$$F - F_0 + \frac{b}{c_1}\dot{F} = c_0 z + b\left(1 + \frac{c_0}{c_1}\right)\dot{z}. \tag{2.18}$$

A coefficient comparison between Eq.(2.15) and Eq.(2.18) provides the link between the thermodynamic and the mechanical model. By regarding the relation: $p_0 V_0 = m_L c_v(\kappa - 1)T_u$ the mechanical parameters can be expressed by thermodynamic parameters in terms of the pressure p_0

$$c_0 = -\frac{J_4}{J_2} = p_0 \frac{{V_1}^2}{V_0} - (p_0 - p_u)V,$$
$$c_1 = -J_3 - c_0 = p_0 \frac{{V_1}^2}{V_0}(\kappa - 1), \tag{2.19}$$
$$b = \frac{J_1}{J_2}c_1 = \frac{\left(p_0 V_1\right)^2}{kAT_u},$$

or the preload F_0 in design-position

$$c_0 = -\frac{J_4}{J_2} = p_u \frac{{V_1}^2}{V_0} + F_0\left(\frac{V_2}{V_1} - \frac{V_1}{V_0}\right),$$
$$c_1 = -J_3 - c_0 = \left(p_u V_1 - F_0\right)\frac{V_1}{V_0}(\kappa - 1), \tag{2.20}$$
$$b = \frac{J_1}{J_2}c_1 = \frac{\left(p_u - \frac{F_0}{V_1}\right)^2 {V_1}^2}{kAT_u}.$$

Comparing Eq.(2.15) and Eq.(2.18) with Eq.(2.14), it becomes evident that the simplified mechanical three-parameter model is restricted to the properties around the design-position. As a result of the

linearization, the non-linear characteristic is lost, but the dynamic characteristic can be modeled in a simple manner.

2.4. Analytical solution of the three-parameter model

The dynamic transfer characteristic of technical systems is usually presented in the frequency domain. In the meaning of the linear system theory Eq.(2.18) to Eq.(2.20) describe a phase-lifting system with PDT_1 behavior and the transfer function

$$C(j\omega) = K_p \frac{1 + j\omega T_v}{1 + j\omega T_1}, \tag{2.21}$$

with the coefficients

$$K_p = c_0,$$

$$T_1 = \frac{mc_v}{kA} = \frac{p_0 V_0}{(\kappa - 1) kAT_u},$$

$$T_v = T_1 \left(1 + \frac{c_1}{c_0} \right).$$

This transfer function can be divided into the explicit expression of stiffness $c(\omega) = |C(j\omega)|$

$$c(\omega) = K_p \frac{\sqrt{1 + \omega^2 T_v^2}}{\sqrt{1 + \omega^2 T_1^2}}, \tag{2.22}$$

and the loss angle $\phi(\omega) = \arg\left(C(j\omega)\right)$

$$\phi(\omega) = \arctan\left[\frac{\omega\left(T_v - T_1\right)}{1 + \omega^2 T_1 T_v} \right]. \tag{2.23}$$

K_p is the proportional gain and corresponds to the stiffness c_0 of the analogous model (see Fig.4). In the quasi-static borderline case for low frequencies, the transfer function $C(j\omega \to 0)$ is reduced to this gain. The change of the inner temperature T is totally compensated by the heat transport across the system border. Hence, the thermodynamics proceeds isothermally for low velocity and c_0 is the isothermal or quasi-static stiffness c_{stat}

$$c_{stat} = c_0 = p_0 \frac{V_1^2}{V_0} - \left(p_0 - p_u\right) V_2. \tag{2.24}$$

For high frequencies $j\omega \to \infty$, the first part in Eq.(2.21) can be neglected. The transfer function corresponds to the sum of the two stiffnesses $c_0 + c_1$. The high velocity of the suspension process disables

the heat transport across the system border. Consequently, the thermodynamics proceeds adiabatically with the dynamic stiffness c_{dyn}

$$c_{dyn} = c_0 + c_1 = \kappa p_0 \frac{V_1^2}{V_0} - \left(p_0 - p_u\right) V_2. \tag{2.25}$$

From Eq.(2.24) and Eq.(2.25), it is evident that only in the special case $V_2 \to 0$ the ratio of dynamic (adiabatic) and static (isothermal) stiffness corresponds to the isentropic exponent κ as shown by Pelz and Buttenbender (2004)

$$V_2 = 0 \to \quad \frac{c_{dyn}}{c_{stat}} = 1 + \frac{c_1}{c_0} = \kappa. \tag{2.26}$$

From a mechanical point of view, both cases can also be deduced from the three-parameter model in Fig.4. For slow displacements, the dashpot element *b* behaves like an ”endlessly” flexible body. So the spring element c_1 decouples completely from the spring movement and only the spring element c_0 gains the force. For a sufficiently high velocity, the dashpot behaves like a rigid body and the force is also gained by the c_1 element. Consequently, both springs are in parallel connection.

The complete course of the transfer function from Eq.(2.21) is shown in the Bode diagram in Fig.5. Additionally, the equivalent Nyquist plot of the complex solution is given. In Fig.5b it can be seen that no phase shift occurs between the displacement and response force on the outer limits. Consequently, the corresponding values of the Nyquist plot are completely on the real parts and the thermodynamics theoretically occurs reversibly for these frequencies.

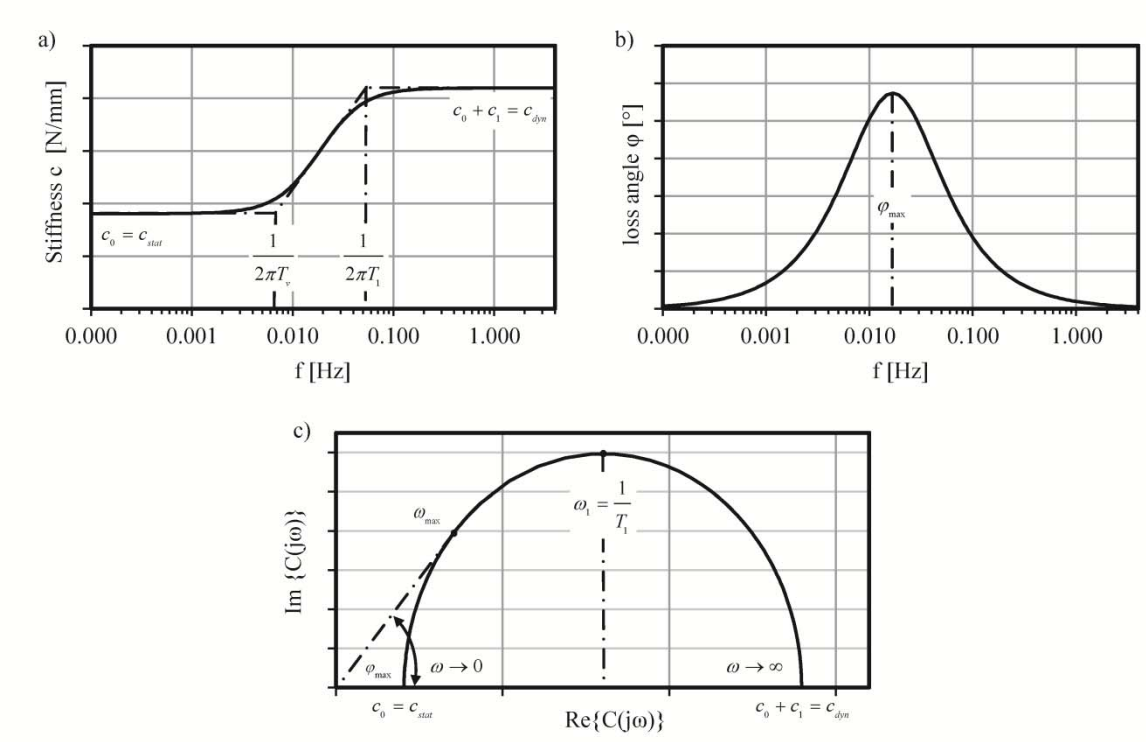

Fig.5. Bode diagram for (a) stiffness; (b) loss angle and (c) Nyquist plot of an air spring.

The occurring phase shift in the transfer and the associated damping is determined by the time constants T_1 and T_v. Both time constants depend on each other and are defined by the heat transmission coefficient kA (see Eq.(2.21)). From a mechanical point of view, the damping seems to be viscous in character. However, the mechanism is not the change of kinetic energy into heat as a result of inner friction, but rather the heat transmission from air volume to the environment.

3. Simulation and validation

To estimate the validity of the previous equations the dynamic system behavior of a passenger car air spring (presented in Fig.6) is simulated in this section. This air spring is designed with a very thin sleeve $(\delta \leq 2\,mm)$ with a single axial fiber layer. The influence to the overall stiffness can be neglected for this design. Additionally, the outer support fulfills the previously discussed neglecting of volume dependence affected by pressure change. The corresponding measurements were made without damper and jounce bumper to get the pure air spring characteristics. The material values used for the simulation are summarized in Tabs 1-4. Comments to the parameter assignments are given in the Appendix.

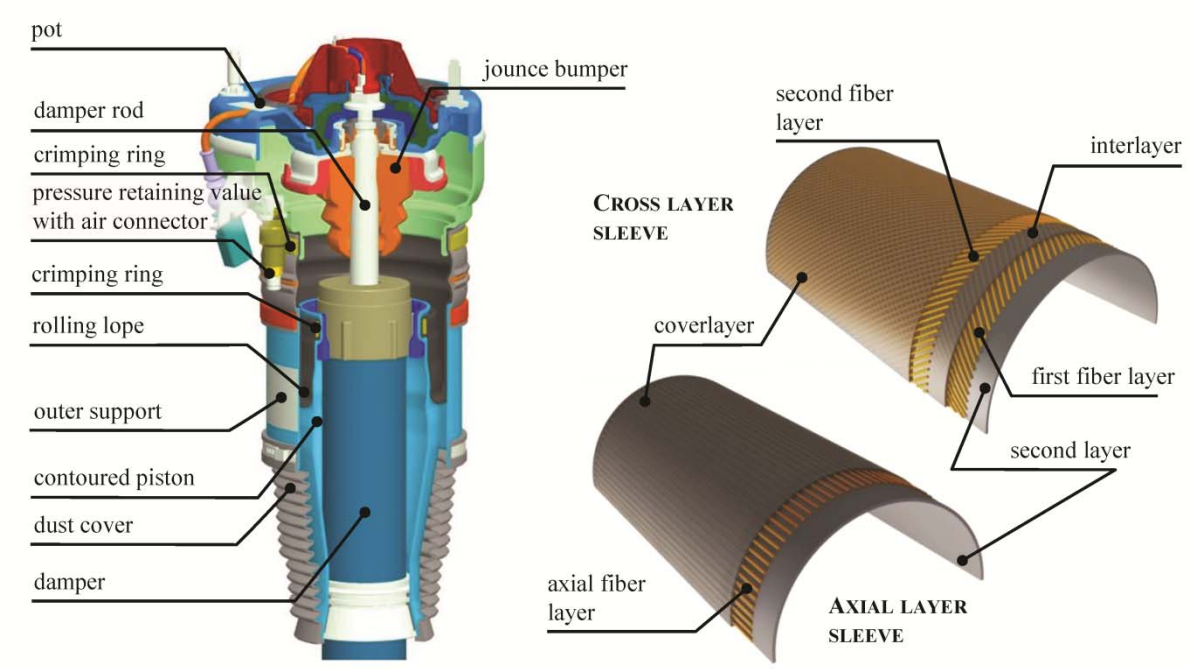

Fig.6. (a) Components of an air spring (Audi A8 suspension strut) (TBVC, 2013); (b) bellows structure of axial and cross layer bellows.

Equation (2.5), Eq.(2.9) and Eq.(2.11) build the non-linear thermodynamic model. It is numerically solved in MATLAB Simulink. Therefore it is difficult to access the interaction of different parameters regarding the overall system behavior. This access is the great advantage of the mechanical three-parameter model (Eq.(2.18) to Eq.(2.20)).

The dynamic transfer characteristic of technical systems is usually presented in the frequency domain (see Fig.5). In contrast to the mechanical three-parameter model, the frequency responses of the thermodynamic model and measurements can only be determined indirectly from the non-linear hysteresis. The process applied here is based on the method described by Puff (2009) for evaluating air spring

characteristic curves. To determine a representative stiffness $c(\omega)$, the average tangent-stiffnesses of the upper and lower flanks are taken.

Table 1. Material data according to Giek (1995).

	$\lambda\,[W/mK]$	$c\,[J/kgK]$	$\rho\,[kg/m^3]$
Upper mounting (cover)	*50*	*510*	*7900*
Axial bellow	*0.2*	*1800*	
Outer support & piston	*204*	*879*	*2600*

Table 2. Material data for air as an ideal gas according to Baehr (2008).

$p_0\,[bar]$	$T_0 = T_u\,[K]$	$R\,[J/kgK]$	$c_v\,[J/kgK]$
9.2	*300*	*287.09*	*717.71*

Table 3. Volume-parameter according to Fig.10.

$V_0\,[m^3]$	$V_1\,[m^2]$	$V_2\,[m]$
$2.26\cdot10^{-3}$	$-9.01\cdot10^{-3}$	$7.84\cdot10^{-3}$

Table 4. Heat transfer coefficients and effective surfaces according to Fig.9.

	$\alpha\,[W/m^2K]$	$\delta\,[m]$	$A_1^1\,[m^2]$	$A_1^2\,[m^2]$	$A_2^1\,[m^2]$	$A_2^2\,[m^2]$	$kA\,[W/K]$	$kA^*\,[W/K]$
Upper mounting	*17.5*	$2.5\cdot10^{-3}$	$2.14\cdot10^{-2}$	$2.01\cdot10^{-2}$	$4.65\cdot10^{-2}$	$4.92\cdot10^{-2}$	*0.97*	*2.73*
Axial bellow	*13.1*	$1.8\cdot10^{-3}$			$3.68\cdot10^{-2}$	$3.79\cdot10^{-2}$		
Outer support	*11.6*	$1.5\cdot10^{-3}$			$3.79\cdot10^{-2}$	$3.89\cdot10^{-2}$		
Piston	*15.5*	$2.0\cdot10^{-3}$	$5.15\cdot10^{-2}$	$5.67\cdot10^{-3}$	$3.34\cdot10^{-2}$	$3.56\cdot10^{-2}$		

The area enclosed by the hysteresis corresponds to the energy dissipated per cycle. With the hysteresis width $h_b(\omega)$, the average stiffness $c(\omega)$ and the amplitude of displacement $\hat{z}$, an approximation by an ideal elliptical hysteresis leads to the determination of the loss angle

$$\phi(\omega) \approx \arcsin\left(\frac{h_b(\omega)}{2c(\omega)\hat{z}}\right). \tag{3.1}$$

Figure 7 shows the Bode diagram of the two models and the corresponding measurement. The numerical solution of the thermodynamic model is in particular very close to the measurement. The characteristic cut-off frequency of the damping maximum is *0.025* Hz. The curve of the linear three-parameter model is shifted to lower frequencies. Due to the simplification of heat transfer, the model predicts a damping maximum at *0.006* Hz. However, accurate frequency responses can be reached by using an empirical gain of the effective heat transfer $kA \rightarrow kA^*$ (see Tab.4). So fortunately the necessary simplifications of the heat transfer can be simply adjusted.

Regarding the graph in Fig.7a, the simulated values are little but evidently below the measured values. The difference of $\approx 1.5\ N/mm$ is in good agreement with the expected single bellow elasticity. A high correspondence occurs for the loss angle at the damping maximum. But beside the maximum the predicted values fall increasingly below the measurement. The neglect of the damping of the elastomeric bellow may cause this deviation. In the simulations, only the damping due to the thermodynamics is considered. Therefore no hysteresis arises in the isothermal and adiabatic borderline cases. However, in measurements of air springs the damping of the bellow is always superimposed.

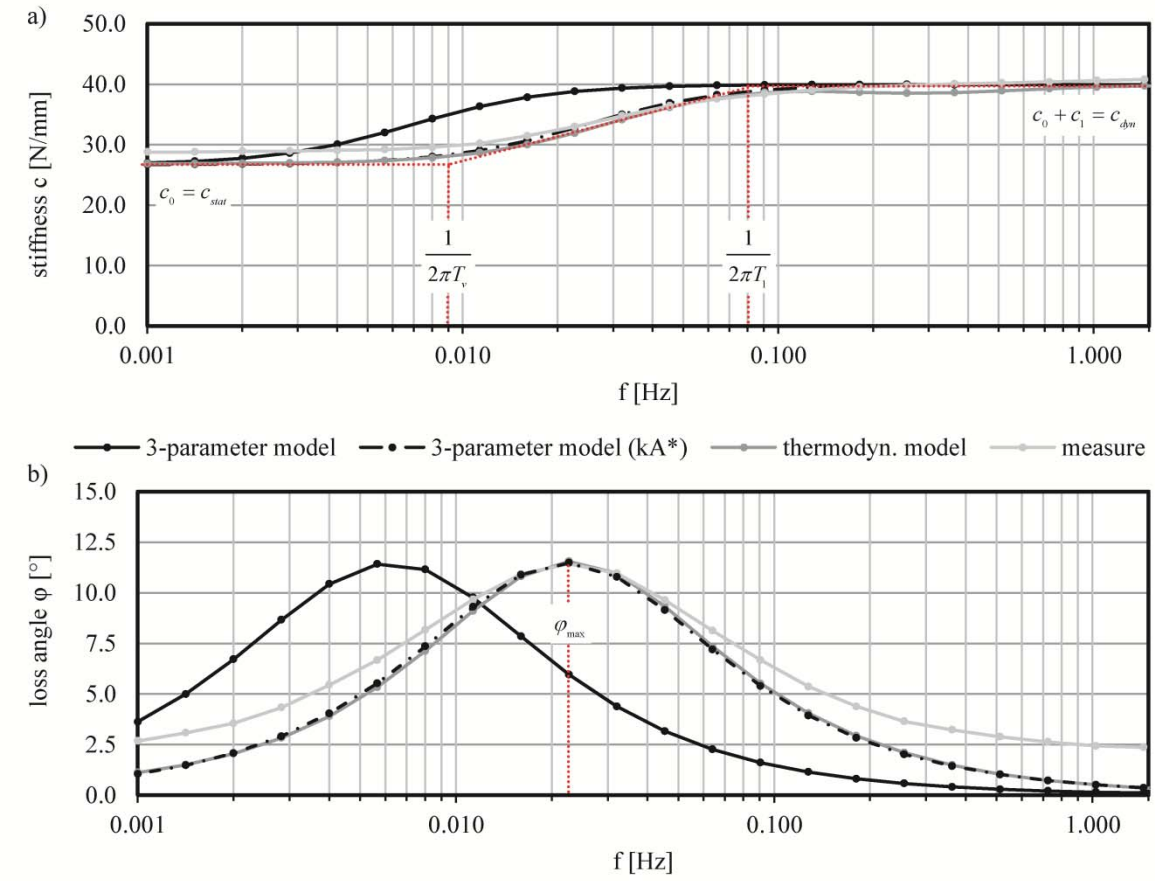

Fig.7. Bode diagram (a) stiffness and (b) loss angle of the simulated model versions.

Additionally to the frequency domain, Fig.8 shows three complete hystereses from the time domain. A very good correspondence between the thermodynamic model and the measurements is confirmed. The three-parameter model corresponds to linearization; consequently a purely elliptical hysteresis shows up and the non-linear characteristic curve is absent, but the hysteresis and stiffness increase are still accurate.

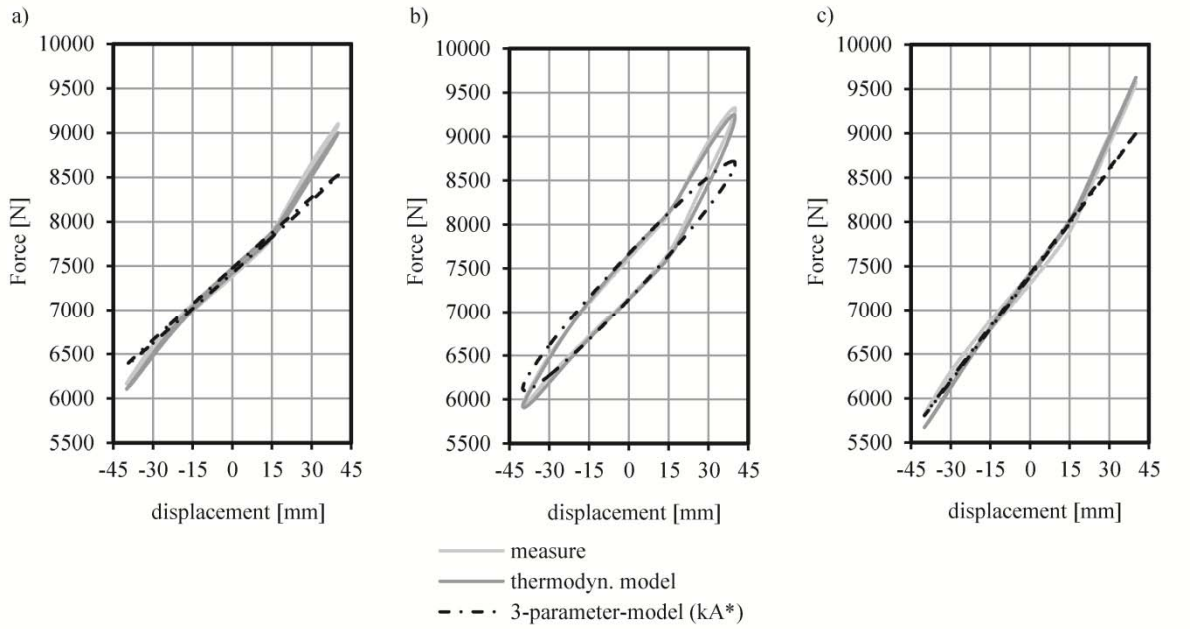

Fig.8. Comparison of the simulated and measured characteristic curves: (a) *0.001* Hz; (b) *0.022* Hz; (c) *1.024* Hz.

4. Conclusion

The stiffness and hysteresis of an air spring were examined in this work. At first a thermodynamic model, based on energy exchange between the air volume, the mountings and the environment is given. A very good correspondence between simulation and measured hysteresis of a passenger car air spring can be confirmed. All parameters of the model are expressed by physical constants and geometrical information. No fitting procedure is needed. The thermodynamic expression describes a non-linear and coupled differential system with time dependent volume and pressure functions. These equations can be simplified into a pure mechanical force-displacement law. However, still no analytic solution can be found. So, finally linearization around the design-level leads to an equivalent representation comprising two springs and one dashpot in a specific arrangement. With this analogy the non-obvious dynamical behaviour of an air spring can be explained quite simply from a mechanical point of view. While the hysteresis formation of a damper ought to be familiar to every engineer, it is not immediately obvious why an air spring likewise demonstrates viscous damping according to the hysteresis.

Acknowledgements

The authors would like to thank Tom Forke and Thorsten Brüger from TrelleborgVibracoustic for taking the measurements and the financial support of the scientific project. Also the authors thank (Prof.) Frank Mantwill for his scientific contribution.

Nomenclature

A_w – effective surface

A_1^i, A_2^i, A_m^i – effective surfaces, average surface of the i'th mounting element for reduced heat transfer

b – coefficient of the linear dashpot element

$C(j\omega)$ – complexe transfer function of an air spring
c_0, c_1 – coefficient of the linear spring elements
c_i – heat capacity of of the *i*'th mounting element
c_{in}, c_{out} – heat capacity in the in- and output mass transport
c_v – heat capacity of air as an ideal gas
$c(\omega)$ – frequency depending stiffness of an air spring
F – air spring force
F_0 – preload of an air spring
h_{in}, h_{out} – heat content in the in- and output mass transport
$\boldsymbol{J}$ – Jacobian Matrix
J_1, J_2, J_3, J_4 – coefficients of the Jacobian Matrix $\boldsymbol{J}$
K_p – proportional gain in the transfer function $C(j\omega)$
kA – heat transmission coefficient
$k_i A_i$ – heat transmission coefficient of the *i*'th mounting element
m, m_L – mass of the air volume V
m_i – mass of the *i*'th mounting element
m_{in}, m_{out} – masses of the in- and output mass transport
P_{ext} – external power transfer
p, p_u – internal pressure in the air volume V, ambient pressure
Q – thermal energy in the air volume V
R – specific gas constant of air
T, T_u – temperature of the enclosed air volume V, ambient temperature
T_{wi} – average wall temperature of the *i*'th mounting element
U – internal energy of the enclosed air volume V
V – enclosed air volume
V_0 – design volume of an air spring
V_1, V_2, V_3 – Taylor coefficients of the volume function $V(z)$
$\boldsymbol{x_0}$ – vector for linearization
z – displacement in *z*- direction
α – heat transfer coefficient
α_1^i, α_2^i – heat transfer coefficient for reduced heat transfer
δ_i – wall thickness of the *i*'th mounting element
κ – isotropic exponent of air
λ_m^i – average heat conductivity of the *i*'th mounting element
$\phi(\omega)$ – frequency depending loss angle of an air spring

Appendix A: Comments to parameter assignment

To enable the simulation, all necessary parameters can be estimated from physical constants and geometrical information. No fitting process is needed. The determination of the *kA* factor (see Eq.(2.8)) requires an effective surface area. This area can be estimated by regarding the geometry as idealized bodies with rotatory symmetry. Figure 9 shows the geometry of the components idealized by the two simplified basic forms of a flat circle area and hollow cylinder. Thus the needed average areas can be determined by analytical equations of the individual areas

$$A_m = \frac{(A_1 + A_2)}{2} \quad \text{(flat circle area)}$$
$$A_m = \frac{(A_2 - A_1)}{\ln\left(\frac{A_2}{A_1}\right)} \quad \text{(hollow cylinder).} \tag{A.1}$$

The specific material values: heat conductivity λ, specific heat capacity c and density ρ‡ for solid bodies and gases can be determined directly from table reference literature and standard literature like (Baehr, 2008; Giek, 1995).

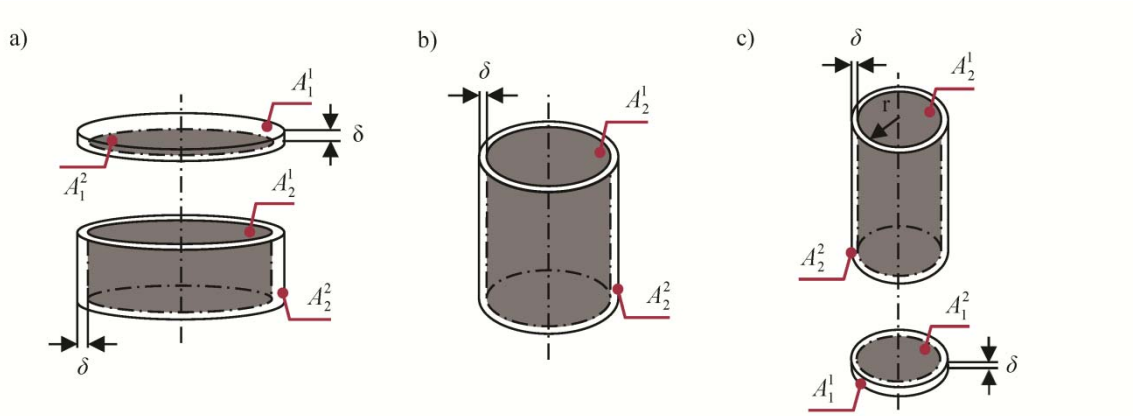

Fig.9. Simplified rotationally symmetrical basic forms: (a) cup; (b) bellow and outer support; (c) piston.

The heat transfer coefficient α_i depends on the component geometry and flow conditions apart from the material. As a result, they cannot be determined directly as constant material values from table reference works (DIN EN ISO 6946). For this reason, the transfer coefficients were determined using cooling over time measurement for free convection of a single bellow

$$\frac{T(t) - T_u}{T_0 - T_u} = e^{-\left(\frac{\alpha_i A_{wi}}{m_i c_i}\right)t}. \tag{A.2}$$

The temperatures T_0 and T_u are the initial temperature of the heated component and the constant ambient temperature. The other variables are according to the material values listed in Tab.1.

At least the volume function $V(z)$, displacement area dV/dz and the coefficient d^2V/dz^2 can be directly determined by geometrical consideration of the piston shape. Fig.10 shows the curves corresponding to the air spring, presented in Fig.6. In the design-position $(z=0)$, the function values correspond to the parameters V_0, V_1 and V_2 of the linearized system from Eq.(2.15). The values used for the three-parameter model are listed in Tab.3. For the thermodynamic model the volume function $V(z)$ and its derivation dV/dz from Figs 10a, b are completely deposited as discreet look-up tables. Because of

‡ In gases, the density depends on the temperature or the thermodynamic condition of the gas. For this reason, the mass of the air volume here was determined using the ideal gas law.

the outer support in the presented example the volume functions can be deduced by constitutive geometrical equations based on rotation integrals. But in consequence of the extensive derivation and focusing the transfer from a thermodynamic to a mechanical system in this work, the procedure is not being explained in detail. For further information the works by Prasil *et al*. (2005; 2006) present a geometric approach for convoluted and multi-convoluted air springs (see. Fig.1a), based on differential equations.

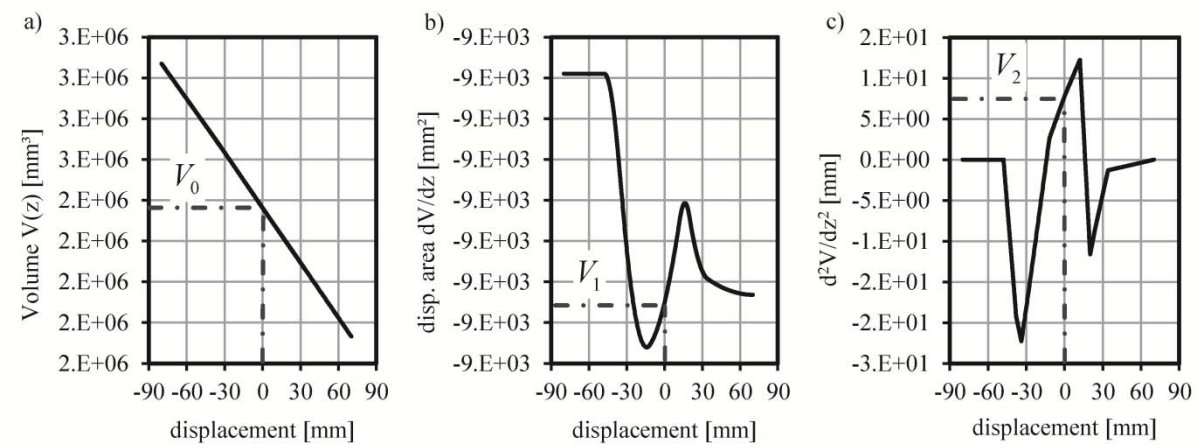

Fig.10. Associated (a) volume function $V(z)$; (b) displacement area dV/dz; (c) volume coefficient d^2V/dz^2.

References

Baehr H. (2008): *Wärme- und Stoffübertragung*. – Berlin: Springer Publishing Company.

Chang F. (2008): *Dynamic model of an air spring and integration into vehicle dynamics model*. – Proceedings of the Institution of Mechanical Engineers-Part D: J. Automobile Engineering, vol.222, pp.1813-1825, London.

DIN EN ISO 6946, Bauteile - Wärmedurchlasswiderstände und Wärmedurchgangskoeffizienten – Berechnungsverfahren, German Institute for Standardization, Beuth Publishing Company, Berlin (2008)

Giek K. (1995): *Technical Formulae*. – Gieck Publishing Company, Germering.

Kornhauser A.A. and Smith J.L. (1993): *The effects of heat transfer on gas spring performance*. – Journal of Energy Resources Technology, vol.115, pp.70-75, London.

Kornhauser A.A. (1994): *Dynamic modeling of gas springs*. – Journal of Dynamic Systems - Measurement and Control, vol.116, pp.414-418, London.

Lee J. and Kim K. (2007): *Modeling of nonlinear complex stiffness of dual-chamber pneumatic spring for precision vibration isolations*. – Journal of Sound and Vibration, vol.301, pp.909-926.

Maßmann C. (1995): *FE-Berechnung an Cord-Gummi Verbundwerkstoffen zur Ermittlung von Ermüdungsmechanismen in Luftfedern*. – KGK Kautschuk Gummi Kunstoffe, vol.48, pp.423-429.

TBVC. (2013): Internal documents, with kind permission of Trelleborg Vibracoustic GmbH & Co. KG, Hamburg.

Pelz P. (2007): Beschreibung von pneumatischen Dämpfungssystemen mit dimensions-analytischen Methoden. – VDI Report 2003, pp.289-304.

Pelz P. and Buttenbender J. (2004): *The dynamic stiffness of an air-spring*. – ISMA 2004 International Conference on Noise and Vibration Engineering, Leuven.

Pelz P., Böcking J., Oberle R.V., Brook U. and Jaschke H. (2002): Simulation eines Luft – Feder - Dämpfers (LFD). – VDI Report 1701.

Pelz P., Böcking J., Oberle R.V., Brook U. and Jaschke H. (2002): Simulation eines Luft – Feder - Dämpfers (LFD). – VDI Report 1701.

Prasil L., Kracik V. and Frydrych D. (2005): *Shape modelling of air bellows springs*. – Proceedings of Algoritmy, pp.914-926, Podbanske.

Prasil L., Kracik V. and Frydrych D. (2006): *Contact problem in shape modelling of multi-bellows air springs*. – Proceedings of the 6th WSEAS International Conference on Simulation, Modelling and Optimization, pp.487-491, Lissabon.

Puff M. (2009): *Entwicklung einer Prüfspezifikation zur Charakterisierung von Luftfedern*. – Report Fluidsystemtechnik, Technische Universtität Darmstadt.

Schützner P., Glasner E. and Povel R. (1994): *Thermodynamische Analysen von Luftfedersystemen*. – VDI-Report 1153, pp.113-135.

Quaglia G. and Sorli M. (2001): *Air suspension dimensionless analysis and design procedure*. – Vehicle System Dynamics, vol.36, pp.443-475.

Voß H. (1988): *Die Luftfederung, eine regelbare Fahrzeugfederung*. – Continental AG, Hannover.

Welsch M. (2007): *Der Einfluss der Rollbalgkonstruktion auf die Charakteristik einer Luftfeder*. – Hamburg: University of Applied Science Hamburg (HAW).

Received: May 7, 2014

Revised: December 9, 2014